Results on longitudinal spin physics at COMPASS

Malte Wilfert[a,1,*], on behalf of the COMPASS Collaboration

[a] *Universität Mainz, Institut für Kernphysik, Johann-Joachim-Becher-Weg 45, D 55128 Mainz*

Abstract

The COMPASS experiment at the CERN SPS has taken data for deep inelastic scattering of polarised muons off a polarised NH_3 target in 2007 and 2011 and off a polarised ^{6}LiD target in 2002-2004 and 2006.
We present our new results on the longitudinal double spin asymmetry A_1^p and the spin-dependent structure function g_1^p obtained from the 2011 data set. These results are used in a NLO QCD fit to the world data to obtain the polarised parton distributions. Also an update on our results on the Bjorken sum rule, connecting the integral of the non-singlet spin-dependent structure function with the ratio of the weak coupling constants, is given.
The gluon polarisation can be accessed directly via the photon gluon fusion process in semi-inclusive deep inelastic scattering. This process is studied using the p_T dependence of charged hadron asymmetries. The latest results indicate a positive gluon polarisation in the kinematic region of COMPASS.

Keywords: COMPASS, deep inelastic scattering, spin, A_1 , g_1 , structure function, polarised parton distribution functions, QCD analysis, Bjorken sum rule, A_{LL}, ΔG

1. Introduction

The COMPASS experiment at CERN aims at exploring the spin structure of the nucleon. For this the spin-dependent structure function g_1 is of special interest; especially as the quarks contribute only roughly 30% to the nucleon spin. Performing the QCD analysis of the world data on g_1 gives access to the helicity distributions of quarks and gluons. Furthermore it is possible to verify the Bjorken sum rule.The gluon polarisation ΔG can also be extracted using a different method where the longitudinal semi-inclusive double spin asymmetry is used. In semi-inclusive processes also the photon-gluon fusion contributes, which gives direct access to the gluon polarisation.
The data were recorded at the COMPASS experiment at the M2 beam line of the CERN SPS in the years 2002 - 2006 using a polarised ^{6}LiD target; in 2007 and 2011 a polarised NH_3 target was used. In 2011 the energy of the polarised muon beam has been increased from 160 GeV to 200 GeV to extend the acceptance towards lower values of x and higher values of Q^2.

2. Experiment

A detailed description of the experiment can be found in Ref. [1]. The target used in the COMPASS setup in 2011 consists of three oppositely polarised cells. Therefore scattering on targets of both polarisation directions can be measured simultaneously. Rotating the solenoid field of the target results in a simultaneous changing the polarisation of all target cell. This gives a better cancellation of the luminosity and acceptance differences in asymmetry calculations.

3. Results on A_1^p and g_1^p

For the extraction of the longitudinal photon-nucleon double spin asymmetry a simultaneous measurement with both target polarisations is performed. To obtain the final value of the photon nucleon double spin asymmetry A_1 the target polarisation, the beam polarisation, the dilution factor and the depolarisation factor have to be employed. The new results for A_1 can be directly converted into the spin dependent structure function g_1 as the contributions from A_2 are negligible in the COMPASS kinematic region, *i.e.* $g_1 = F_2/(2x(1+R))\,A_1$. The results for g_1^p from the 2011 data taking are shown in Figure 1 as function of Q^2 for different values of x together with the world data. Also the result of our NLO QCD fit and its uncertainty is shown.

*Speaker
Email address: mwilfert@cern.ch (Malte Wilfert)
[1] Supported by BMBF and GRK Symmetry Breaking

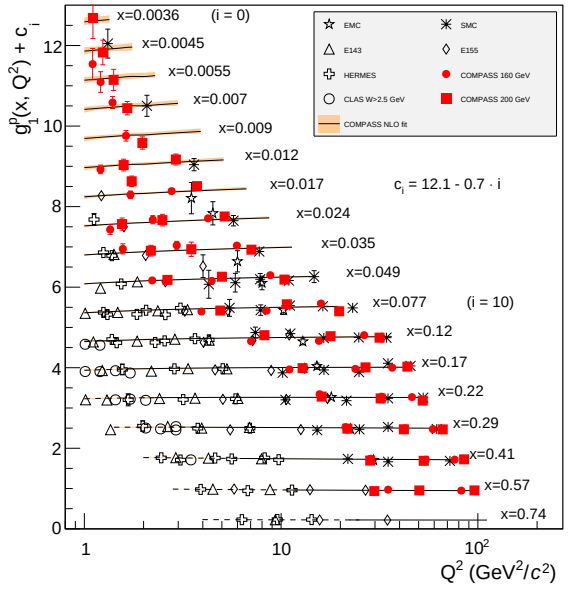

Figure 1: World data on g_1^p as a function of Q^2 for different x. The solid line represents the result of our NLO QCD fit. The dashed line indicates an extrapolation for $W^2 < 10\ (\mathrm{GeV}/c^2)^2$.

4. QCD fit to the world data

The new COMPASS results on g_1^p are used together with the world data on g_1^p, g_1^d and g_1^n in the DIS region, $Q^2 > 1\ (\mathrm{GeV}/c)^2$, in a NLO QCD fit. To avoid possible effects due to higher twists a cut on $W^2 > 10\ (\mathrm{GeV}/c^2)^2$ is applied to the data. The kinematic coverage of the data is shown in Figure 2. The shown data are from EMC [2], SMC [3], SLAC E143 [4], SLAC E155 [5], HERMES [6], COMPASS [7] and CLAS [8] for the proton data; from SMC [3], SLAC E143 [4], SLAC E155 [9], HERMES [6], COMPASS [10] and CLAS [8] for the deuteron data and from SLAC E142 [11], SLAC E154 [12], JLab Hall A [13] and HERMES [14] for the ^{3}He data.

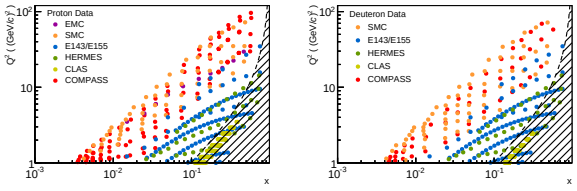

Figure 2: Kinematic coverage of the g_1^p and g_1^d world data. The hatched area indicates the region with $W^2 < 10\ (\mathrm{GeV}/c^2)^2$.

The fit, which is performed in the $\overline{\mathrm{MS}}$ renormalisation and factorisation scheme, uses the DGLAP equations to describe the Q^2 dependence of the singlet distribution Δq^S, the gluon distribution Δg and the two non-singlet distributions Δq_3 and Δq_8. As the DGLAP equations only describe the Q^2 dependence and no x dependence a parametrisation has to be used at a reference scale Q_0 that is chosen to be $Q_0^2 = 1\ (\mathrm{GeV}/c)^2$. The functional form is:

$$\Delta q_i(x) = \eta_i \frac{x^{\alpha_i}(1-x)^{\beta_i}(1+\gamma_i x)}{\int_0^1 x^{\alpha_i}(1-x)^{\beta_i}(1+\gamma_i x)\mathrm{d}x}, \qquad (1)$$

where $i = S, g, 3, 8$ and η_i are the first moments of each distribution at the reference scale. In case of the non-singlet distributions these are fixed via the baryon decay constants $\eta_8 = F + D$ and $\eta_3 = 3F - D$, for these distributions also γ_i is fixed to zero as it is not well constrained and not needed to describe the data. In case of the gluon distribution γ_g is also fixed to be zero for the same reason. In addition also β_g is fixed to the corresponding value of the unpolarised distribution taken from MSTW [15]. In each step during the fit it is checked that the positivity constrain $|\Delta q(x)| < q(x)$ is valid using the unpolarised parton distributions from MSTW [15] for u, d, s and g. An extra term penalising possible violations is added to the χ^2. For this version of our QCD fit a special interest was put in the systematic uncertainties. We tested different parametrisations of the singlet and gluon distribution, also ones which use more parameters as shown above. The largest contribution to the systematic uncertainty comes from the dependence on the reference scale. This has been studied by performing multiple fits where we have changed the input scale from $Q_0^2 = 1\ (\mathrm{GeV}/c)^2$ to $Q_0^2 \approx 70\ (\mathrm{GeV}/c)^2$. This is illustrated in Figure 3 for one of our solutions.

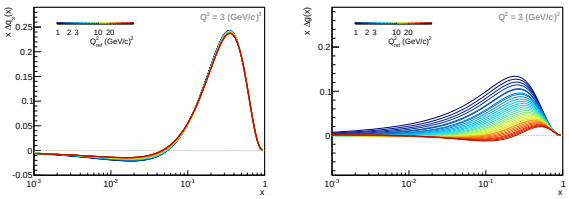

Figure 3: Dependence on the reference scale Q_0 for one of our solutions. The left plot shows the influence on the singlet distribution and the right one the influence on the gluon distribution.

The result from all studies is that there are two kinds of functional shapes that describe the data equally well with similar χ^2/NDF. For one solution γ_S is also fixed to zero resulting in a negative gluon distribution; for the other solution γ_S is a free parameter resulting in a posi-

tive gluon distribution. The final result is shown in Figure 4.

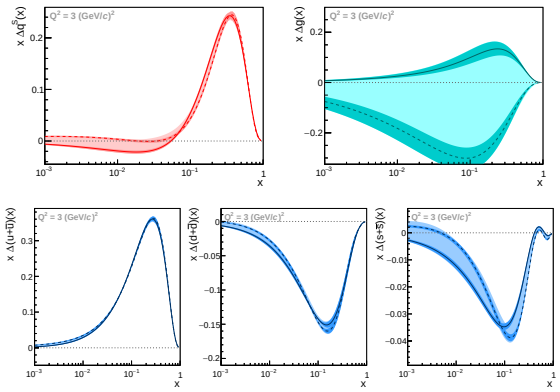

Figure 4: Result of the QCD fit to the world data. The solid lines indicate our two solutions with their statistical uncertainties indicated as a darker band. The lighter band corresponds to the combined systematic and statistical uncertainty of the fit.

From the fit the first moment of the singlet distribution, the contribution of the quarks to the total spin of the nucleon is estimated to be $0.26 < \Delta\Sigma < 0.36$. Using the fit the gluon polarisation ΔG is not well constrained. To get access to ΔG another kind of measurement is needed.

5. Bjorken sum rule

The QCD fit can also be used to evaluate the Bjorken sum rule, which connects the first moment of the non-singlet structure function

$$g_1^{NS}(x, Q^2) = g_1^p(x, Q^2) - g_1^n(x, Q^2) \qquad (2)$$

with the ratio of the weak coupling constants

$$\Gamma_1^{NS}(Q^2) = \int_0^1 g_1^{NS}(x, Q^2)\mathrm{dx} = \frac{1}{6}\left|\frac{g_A}{g_V}\right| C_1^{NS}(Q^2), \qquad (3)$$

where $C_1^{NS}(Q^2)$ is the non-singlet coefficient function, which has been calculated in perturbative QCD [16]. To calculate the first moment only the COMPASS data are used which are evolved to the Q^2 of the 2007 data using the results from the NLO QCD fit and are later combined to get g_1^{NS}. Afterwards a second NLO QCD fit is performed to fit the non-singlet structure function, which requires only the non-singlet distribution Δq_3 to describe the data. The program is the same as used in the fit of the g_1 world data. The results are used to evolve the non-singlet structure function to a common Q^2 of $3\,(\mathrm{GeV}/c)^2$. A comparison of our data and the non-singlet fit is shown in Figure 5. To evaluate the first moment also an extrapolation to the unmeasured region is needed ($x < 0.0025$ and $x > 0.7$). These contributions are evaluated using the results from the non-singlet fit. The dependence of the first moment Γ_1^{NS} on its lower limit is shown in Figure 6. The result for

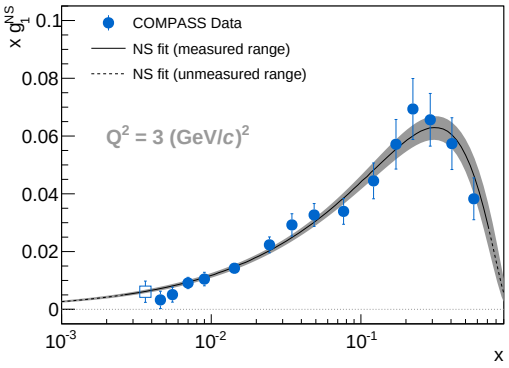

Figure 5: Values of g_1^{NS} at $Q^2 = 3\,(\mathrm{GeV}/c)^2$ compared to the NLO fit. The open square corresponds to the data point where the deuteron contribution is taken from the NLO QCD fit.

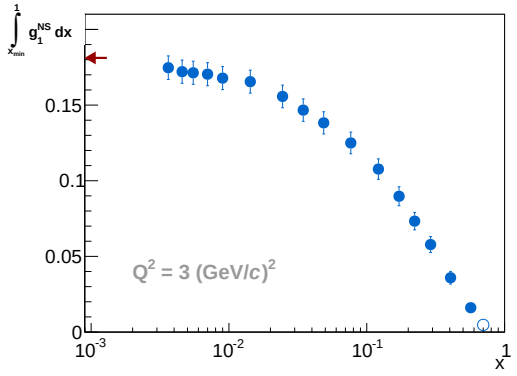

Figure 6: Dependence of the first moment Γ_1^{NS} as a function of x_{min}. The open circle at $x = 0.7$ is obtained from the fit. The arrow on the left side indicates the value for the full range $0 < x < 1$.

the first moment of the non-singlet structure function at $Q^2 = 3\,(\mathrm{GeV}/c)^2$ is

$$\Gamma_1^{NS} = 0.181 \pm 0.008(\mathrm{stat}) \pm 0.014(\mathrm{syst})\,, \qquad (4)$$

where 94% of the first moment are in the measured region. Using the non-singlet coefficient function in NLO the ratio of the weak coupling constants can be extracted

$$\left|\frac{g_A}{g_V}\right| = 1.22 \pm 0.05(\mathrm{stat}) \pm 0.10(\mathrm{syst})\,. \qquad (5)$$

The largest systematic uncertainty is the one from the beam polarisation. Other sources from the target po-

larisation, the dilution factor, the depolarisation factor and F_2 are also taken into account. A comparison with the results from the neutron β-decay, $|g_A/g_V| = 1.2701 \pm 0.002$ [17], provides a validation of the Bjorken sum rule on the level of 9%.

6. LO extraction of ΔG

The NLO QCD fit showed that using only inclusive DIS data A_1 is not sensitive to the gluon polarisation. Therefore a different approach is used to get access to this quantity, namely the p_T dependence of charged hadron asymmetries in semi-inclusive deep inelastic scattering is studied. In addition to the leading process (LP), which does not provide direct access to the gluon polarisation, also two other processes are considered in the asymmetry. These processes are the QCD Compton process (QCDC) and the photon-gluon fusion process (PGF), which gives an access to the gluon polarisation (Figure 7). The semi-inclusive asymmetry is given by:

$$A_{LL}^h = \alpha \cdot A_1^{LO}(x_{Bj}) + \beta \cdot A_1^{LO}(x_C) + \gamma \cdot \Delta g/g(x_g) \quad ,(6)$$

where α, β and γ depend on the partonic cross section asymmetries and on the contribution with which each process contributes. These processes have a different dependence on the transverse momentum p_T of the hadron with respect to the virtual photon, this fact is used to simultaneously extract the gluon polarisation and the LP and QCDC asymmetries. An alternative approach would be to use a model for the LO asymmetries. This approach is described in [18] using the same data.

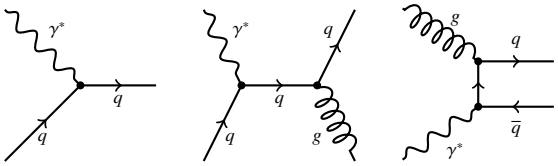

Figure 7: Feynman diagrams for the different processes. Leading-order process (left), QCD Compton (middle) and photon-gluon fussion (right).

The method used to extract the gluon polarisation was introduced in [19] and already used to extract the gluon polarisation from open charm events by using the signal over background ratios for reconstructed D mesons. Here a neural network (NN) is trained using simulated data to give expectation values for the fractions R_i, values of x_i and the partonic cross section asymmetries a_{LL}^i (here i runs over the three simulated processes, LP, QCDC and PGF). The input parameters for the NN are Q^2, x_{Bj}, and the longitudinal p_L and transverse momentum p_T of the leading hadron. Figure 8 shows the kinematic dependence of the three processes on the input parameters. The LP contribution is dominant at low p_T and low y whereas the QCDC component is dominant at high p_T and higher Q^2 and y and the PGF process is dominant at high p_T and high y but at lower Q^2.

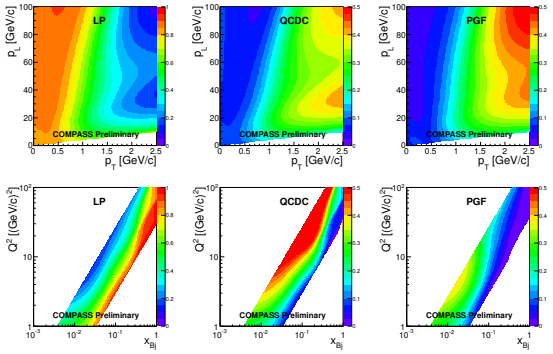

Figure 8: Dependence of different processes on the kinematic variables used as an input for the neural network.

As important quantities are estimated using a Monte Carlo simulation a good description of the detector and the physics is needed. The simulation uses the LEPTO event generator [20] to generate an spin-independent MC sample of events. The detector simulation is done in a GEANT3 based program and the reconstruction is performed in the same way as for real events. A comparison between real data and MC data is shown in Figure 9. The largest differences are found at low p_T, where the LP is dominant and therefore the discrepancy between data and MC has a negligible impact on $\Delta g/g$.

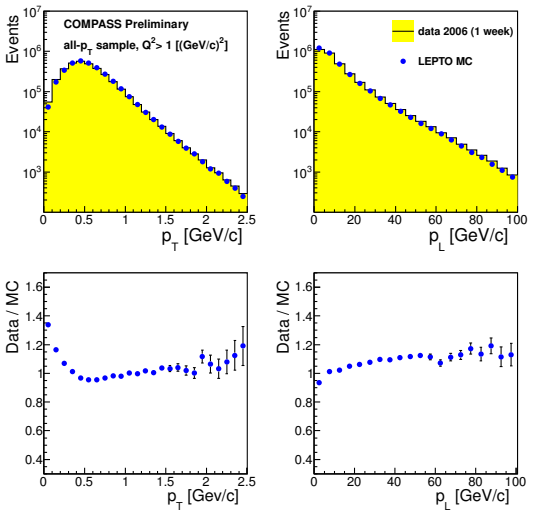

Figure 9: Comparison of the longitudinal p_L and transverse momentum p_T from real data and MC.

The output from the NN is used as weights for each event in a fit to obtain the leading-order asymmetries and also the gluon polarisation. The final result for the gluon polarisation $\Delta g/g$ is:

$$\langle \Delta g/g \rangle = 0.113 \pm 0.038(\text{stat}) \pm 0.036(\text{syst}) \,, \quad (7)$$

which is valid at the scale $\mu^2 = \langle Q^2 \rangle = 3\,(\text{GeV}/c)^2$ and $x_g \approx 0.10$. This is the first direct measurement of a positive value in this region. It is also possible to split up the obtained value in three bins of x_g. A comparison to the world data on $\Delta g/g$ in LO is shown in Figure 10.

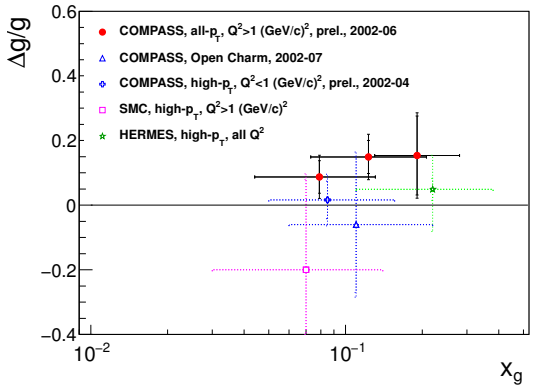

Figure 10: World data on $\Delta g/g$ [21–24] extracted in LO compared to our results in three bins of x_g.

7. Conclusions

The COMPASS data taken in 2011 complete the COMPASS results on the longitudinal double-spin asymmetry A_1^p and allows measuring higher values of Q^2 and lower values of x. These data are used together with the world data on g_1 to extract the polarised parton distributions. The fit results in a range of $0.26 < \Delta\Sigma < 0.36$ for the contribution from the quarks to the total spin of the nucleon. Using only the COMPASS data the result on the Bjorken sum rule has been updated. The resulting ratio of the weak coupling constants is $|g_A/g_V| = 1.22 \pm 0.05 \pm 0.10$, verifying the sum rule within an accuracy of 9%. Additional information on the hadrons in SIDIS allows to extract information on the gluon polarisation in LO, for this a neural network has been trained to disentangle the different contributions to the asymmetry. From this analysis a gluon polarisation of $\langle \Delta g/g \rangle = 0.113 \pm 0.038 \pm 0.036$ is obtained, which is the first direct measurement of a positive gluon polarisation in this kinematic region.

References

[1] COMPASS Collaboration, P. Abbon *et al.* Nucl. Inst Meth. A **577** (2007) 455.
[2] EMC, J. Ashman *et al.,* Phys. Lett. B **206** (1988) 364; Nucl. Phys. B **328** (1989) 1.
[3] SMC, B. Adeva *et al.,* Phys. Rev. D **58** (1998) 112001.
[4] E143 Collaboration, K. Abe *et al.,* Phys. Rev. D **58** (1998) 112003.
[5] E155 Collaboration, P. L. Anthony *et al.*, Phys. Lett. B **493** (2000) 19.
[6] HERMES Collaboration, A. Airapetian *et al.,* Phys. Rev. D **75** (2007) 012007.
[7] COMPASS Collaboration, E. M.G. Alekseev *et al.,* Phys. Lett. B **690** (2010) 466.
[8] CLAS Collaboration, K. V. Dharmawardane *et al.,* Phys. Lett. B **641** (2006) 11.
[9] E155 Collaboration, P. L. Anthony *et al.,* Phys. Lett. B **463** (1999) 339.
[10] COMPASS Collaboration, V. Yu. Alexakhin *et al.,* Phys. Lett. B **647** (2007) 8.
[11] E142 Collaboration, P. L. Anthony *et al.,* Phys. Rev. D **54** (1996) 6620.
[12] E154 Collaboration, K. Abe *et al.,* Phys. Lett. B **79** (1997) 26.
[13] JLab Hall A Collaboration, X. Zheng *et al.,* Phys. Rev. Lett. **92** (2004) 012004.
[14] HERMES Collaboration, K. Ackerstaff *et al.,* Phys. Lett. B **404** (1997) 383.
[15] A. D. Martin *et al*, Eur. Phys. J. C **63** (2009) 189.
[16] S. A. Larin, T. van Ritbergen and J. A. M. Vermaseren, Phys. Lett. B **404** (1997) 153.
[17] J. Beringer *et al* (Particle Data Group), Phys. Rev. D **86** (2012) 010001
[18] COMPASS Collaboration, C. Adolph *et al.,* Phys. Lett. B **718** (2013) 922.
[19] J. Pretz and J.-M. Le Goff, Nucl. Instr. Meth. A **602** (2009) 594.
[20] G. Ingelman, A. Edin and J. Rathsman, Comput. Phys. Commun. **101** (1997) 108.
[21] COMPASS Collaboration, E. S. Ageev *et al.,* Phys. Lett. B **633** (2006) 25.
[22] COMPASS Collaboration, C. Adolph *et al.,* Phys. Rev. D **87** (2013) 052018.
[23] SMC Collaboration, B. Adeva *et al.,* Phys. Rev. D **70** (2004) 012002.
[24] HERMES Collaboration, A. Airapetian *et al.,* Journal of High Energy Physics **1008** (2010) 130.